STUDY OF THERMO-ELECTRO-MECHANICAL COUPLING IN FUNCTIONALLY GRADED METAL-CERAMIC COMPOSITES

A Thesis

by

SUKANYA HARSHAD DOSHI

Submitted to the Office of Graduate Studies of
Texas A&M University
in partial fulfillment of the requirements for the degree of

MASTER OF SCIENCE

Approved by:

Co-Chairs of Committee,	J. N. Reddy
	Anastasia Muliana
Committee Member,	Luciana Barroso
Head of Department,	John Niedzwecki

December 2012

Major Subject: Civil Engineering

ABSTRACT

Piezoelectric actuators have been developed in various forms ranging from discrete layered composites to functionally graded composites. These composite actuators are usually made up of differentially poled piezoelectric ceramics. This study presents analyses of thermo-electro-mechanical response of piezoelectric actuators having combinations of metal and ceramic constituents with through thickness gradual variations of the metal and ceramic compositions. This is done in order to achieve better performance. The piezoelectric ceramic constituent allows for electro-mechanical coupling response and higher resistance to elevated temperatures while the metal constituent provides more ductile composites. The gradual variation in the ceramic and metal composition helps to avoid high stress concentrations at the layer interfaces in composites.

A functionally graded composite is analyzed with discrete layers of piezoelectric ceramic/metal composite. Each layer in the functionally graded composite has a fixed ceramic/metal composition. The governing equation for such a piezoelectric functionally composite beam is presented based on a multi-layer Euler-Bernoulli beam model and the overall displacement response of the beam under thermal, mechanical and electrical stimuli is predicted. The variation of this response is studied with respect to functional grading parameter, number of layers, thermal and electrical and mechanical stimuli

applied. It is found that the displacement due to thermal and mechanical effects can be mitigated to some extent by the application of an electric field. It is also observed that layers of varying thickness may be assumed to model the functional grading more accurately i.e. use thinner layers where the grading changes rapidly and thicker layers where the grading changes gradually. In addition to the above parametric studies, the change in the material properties with temperature is also studied. It is found that the temperature-dependent material parameters are important when the actuators are subjected to elevated temperatures.

ACKNOWLEDGEMENTS

I would like to thank my committee: Dr. Reddy, for his generous leadership; Dr. Muliana for her unceasing direction, helpful mentorship and perpetual support; Dr. Barroso for her constant guidance through this master's program.

The results reported herein were obtained under the National Science Foundation research Grant CMMI-1030836. Their support is gratefully acknowledged.

I'd also like to extend my appreciation to all my colleagues who have helped and guided me throughout my work. My heartfelt gratitude goes out to my family and friends who have been there for me when I most needed them.

NOMENCLATURE

b = Width of beam

$\mathbf{C}$ = Stiffness vector

$\mathbf{d}$ = Piezoelectric strain tensor

$\mathbf{e}$ = Piezoelectric stress tensor

$\boldsymbol{\epsilon}$ = Permittivity Constant

$d_{31} = d$ = Piezoelectric strain coefficient for 31-mode

$\mathbf{E}$ = Electric field vector

E_3 = Electric field in x_3-direction

FGM = Functionally graded material

K = Curvature of beam bending

L = Length of beam

M_2 = External bending moment in y-plane

M_2^T = Bending moment due to thermal stress

M_2^E = Bending moment due to piezoelectric effect

N_1 = External axial load

N_1^T = Axial load due to thermal stress

N_1^E = Axial load due to piezoelectric effect

u_0 = Deformation along x_1-axis

u_1 = x_1-component of total deformation

u_2 = x_2-component of total deformation

u_3 = $w = x_3$-component of total deformation

$Y_1 = Y$ = Young's modulus in x_1 direction

z = Distance of any point on the beam from the neutral axis in the x_3 direction

α = Coefficient of thermal expansion

$\boldsymbol{\varepsilon}$ = Strain vector

ε_0 = Neutral axis strain

$\varepsilon_{11} = \varepsilon_1$ = Normal strain in the x_1-direction

ε_{13} = Transverse shear strain in the x_1x_3 -plane

ε_{22} = Longitudinal strain in x_2-direction

θ = Rotation of a transverse normal to the beam neutral axis

$\boldsymbol{\sigma}$ = Stress tensor

$\sigma_{11} = \sigma$ = Axial stress in x_1 direction

TABLE OF CONTENTS

Page

LIST OF FIGURES

Page

LIST OF TABLES

Page

CHAPTER I

INTRODUCTION AND LITERATURE REVIEW

1.1 Introduction

Piezoelectric actuators are widely used as positioning devices, motors and vibration suppressors. In case of small and lightweight devices, vibration suppression is one of the primary design concerns. In such applications, piezoelectric sensors and actuators are often integrated into structural components to actively reduce vibration of these structures. Another type of actuator/sensor is a piezoelectric bimorph which has been used for precision displacement and volume control and other applications such as positioning devices, motors, pressure sensors, semiconductor chips, optical instruments, bending actuators in textile machines and ink print heads. Piezoelectric actuators have low cost, light weight, high response times, and no electromagnetic noise. Compared to traditional electromagnetic motors, they can have a more compact design and better efficiency [1-3].

A combination of a piezoelectric and an elastic layer, called a unimorph or monomorph was followed by a bimorph type actuator with two piezoelectric layers of opposite polarity. These early forms were developed into other specially designed structures like MOONIE and RAINBOW and further into polymorphs or multilayer bending actuators.

Smits et al. [4] offer a very detailed historical review of the applications and structures of piezoelectric structures.

Smits et al. [4] and Smits and Choi [5] derived the constitutive equations for piezoelectric bimorph beams in case of two antiparallel piezoelectric layers and a combination of piezoelectric and elastic layer, respectively. The energy density function was expressed in terms of stress and electric field as the independent variables. Further, the total energy function was partially differentiated to obtain the intensive properties (displacement, rotation, electric charge) in terms of the extensive ones (applied moment, force and potential difference). Wang and Cross [6] derived similar constitutive equations for a triple layer beam having the central layer made up of an elastic material and the top and bottom being identical piezoelectric layers. The equations provided in these papers are a very useful and convenient way of solving problems related to discrete layered bimorphs. In the above bimorph and unimorph cases, Wang et al. [7] derived an expression for the mechanical energy, the piezoelectric coupling factor and the transmission coefficient as well as their maxima. They found that a stiffer elastic layer leads to better electromechanical coupling. Also, it was found that bending actuators have lower coupling than transverse or longitudinal actuators because internal stresses are built up in the flexural case.

Steel et al. [8] fabricated a bimorph with PZT and Beryllium-Copper as the two components. The tip deflection was found to be proportional to applied voltage and the

square of the bimorph length. Kugel et al. [9] compared the tip deflection, blocked force admittance factor and resonant frequency for various actuator designs: RAINBOW, CERAMBOW, bimorphs and unimorphs and THUNDER. (The layout and origin of these actuators have been provided in the above reference).

A composite material made up of elastic and piezoelectric material may be better tailored towards some specific applications by combining the advantages of both materials. Similarly, a plastic-piezoelectric composite was fabricated by Newnham et al. [10]. This paper also outlines the key concepts to be considered in designing composite piezoelectric structures. In an attempt to improve the behavior of bimorphs, multilayer beams were formed. Based on the work of Marcus [11], it was found that the tip deflection decreased with an increase in the number of layers in a multilayer actuator. This deflection, however, remained a finite value and did not diminish. The internal stress, however, decreased considerably as the number of layers increased. This finding was later supported through the works of [12-16] and many others.

Kouvatov et al. and Hauke et al. [12, 13] conducted an experimental as well as finite element analysis comparing bending in bimorphs and polymorphs. An *n*-layered polymorph was found to agree with Marcus' [11] prediction. The tip deflection reduced with an increase in the number of layers. However, after the number of layers was increased to 11, the deflection was somewhat steady at 70% of the maximum value. The stress however continues to decrease with increasing layers. This is true even with an

increase in the voltage applied. For these studies, a Barium Titanate ceramic was selected. Individual layers were poled separately and glued together. Top and bottom edges had maximum poling. The internal layers were de-poled by in steps order to grade the piezoelectric properties. Taya et al. [17] designed a piezo-composite laminar structure where mirror symmetry of a bimorph was maintained. As in the studies above, the piezoelectric constant was varied functionally. Two configurations were selected – one with the polarization maximum at the center and decreasing toward the outside (type A) while another with the maximum polarization layers toward the outside and decreasing toward the center (type B). The layered models were studied using the classical lamination theory (CLT) to optimize the microstructure to achieve maximum tip displacement and minimum stress field. It was found that the type A was the most optimum design.

Bimorphs provide large displacements, however high stresses are induced at the metal-PZT interface in such actuators possibly causing premature failure. There may also be debonding between the layers in a laminate made up of discrete layers. Therefore, it would be desirable to avoid this debonding while retaining the composite structure. To this end, Wu and Kahn [18] introduced a monomorph in which the piezoelectric property alone had been linearly graded through the thickness. Such graded structures do not cause stress concentration at layer boundaries as do the traditional bimorphs. The study by Taya et al. [17] mentioned above involved functionally grading two piezoelectric materials having different piezoelectric and dielectric properties.

Shi et al. [14] studied piezoelectric and piezo-composite cantilever beams using 2D elasticity. Using a quadratic Airy stress function and a linear induction function, the exact solution was found for a moment couple type loading. This solution was derived for an *n*-layered piezoelectric beam and a 2n layered beam with alternating elastic and piezoelectric structure. The piezoelectric beam was assumed to have a linearly graded piezoelectric constant. This study is particularly useful because it suggests the behavior of a functionally graded material (FGM). Xiang, Shi [15] presented a similar study where the piezoelectric constants were graded non-linearly. The 2D elasticity solution provided was in agreement with the finite element results and the findings in the works of [12, 13]. Once again, the results were in accordance with [11]. Chen and Shi [19] also assumed linearly graded piezoelectric properties. In addition to that, a temperature field varying with thickness was applied giving rise to thermal loads. The cases considered were (1) thermal and electric load, (2) thermal and mechanical load and (3) purely thermal load, (4) purely electrical load. It was found that the combination in case (1) does not induce any stresses in a perfectly graded beam. Case (2) gives rise only to axial stress in the x-direction. The expressions for transverse displacement, longitudinal displacement and potential were derived for the latter two cases. One can also find a brief discussion on the effect of graded thermal and pyroelectric properties. It is predicted that these parameters would not influence the stress distribution. However, there would be a marked difference in the strain distribution, electric field strength and displacement fields.

Functionally graded beams have also been successfully studied in cases where the ceramic is a piezoelectric one (see [20-22]). Zhu and Meng predicted the relationship between the bending displacement and the FGM coefficient based on the principle of minimum potential energy. Huang et al. [20] found that fracture toughness of a PZT/Silver composite depended on the stress relaxation induced by the silver particles. Takagi et al.[21] fabricated a PZT/Pt graded composite and found that the addition of Pt improved the mechanical properties especially the fracture toughness.

In addition to the above studies, there has been extensive research in the field of functionally graded metal-ceramic composites used as thermal barriers. Having lower thermal conductivity, the ceramic provides high temperature resistance while the metal helps provides better mechanical properties in the composite. FGM plates have been studied by Praveen and Reddy (1998), Reddy (2000) and Sankar and Tzeng (2002) [23-25].

1.2 Motivation and Objective

To summarize the past work, the use of piezoelectric materials in the field of actuation has evolved tremendously. In case of composite beams comprising of piezoelectric and composite materials, the electro-mechanical coupling has been extensively studied. Active composite structures with a gradual or discrete variation of the material

properties, termed as active functionally graded structures, promise to be a solution for mitigating stress concentration within layers and avoiding delamination within layers in the smart composite structures.

Several studies involve the grading of solely the piezoelectric properties through the thickness of the actuator by differential poling. Considering the advantages of metal-ceramic composites this study deals with piezoelectric functionally graded composites by combining the piezoelectric ceramic with a non-piezoelectric material (metal). Literature clearly indicates that this would help improve the brittle fracture of such an actuator over a purely piezoelectric ceramic. In addition, the ceramics have high resistance to high temperatures, which make them suitable for high temperature applications. Understanding the overall performance of piezoelectric functionally graded composites under combined thermo-electro-mechanical coupling effects is currently lacking which hinder further development of the piezoelectric functionally graded composites.

This study aims at understanding the thermo-electro-mechanical coupling performance of ceramic-metallic functionally graded piezoelectric beams based on the Euler-Bernoulli beam theory. The through-thickness gradual variation of the thermo-electro-mechanical properties in the functionally graded beam is modeled as discrete layers of ceramic/metal composites with different compositions of the constituents. An analytical model is used to predict the lateral displacement of the piezoelectric functionally graded

beam, undergoing conduction of heat, electric field input, and mechanical loading. Parametric studies are also performed to examine the effect of beam's slenderness ratio, through-thickness material variations, temperature-dependent material properties, and electric and temperature fields applied on the overall performance of the piezoelectric functionally graded beam. The temperature-dependence of material properties are also studied with a view to comment on its impact on the response of such a composite beam.

1.3 Research Tasks

1. Formulate governing equations for the thermo-electro-mechanical coupling in piezoelectric functionally graded cantilever composites based on multi-layered Euler-Bernoulli beam model.
2. Carry out the heat-transfer analysis of the cantilever piezoelectric functionally graded beam for both temperature-dependent and temperature-independent material properties.
3. Predict the overall response of piezoelectric functionally graded composites subject to coupled thermo-electro-mechanical stimuli.
4. Conduct parametric studies to examine the effect of material gradation, temperature-dependent material properties and geometrical aspect ratio on the overall response of piezoelectric functionally graded composites.

CHAPTER II

PIEZOELECTRIC MATERIALS AND ELECTROMECHANICAL COUPLING

2.1 Piezoelectric Materials, Crystal Structure and Domain Switching

Piezoelectricity was discovered in the late 1800s. Based on their studies, Jacques and Pierre Curie proposed that certain crystals generate electric charge when mechanically loaded (known as the piezoelectric effect). Later, this effect was also found to be reversible (inverse piezoelectric effect). As defined by Cady [26], Piezoelectricity is the "electric polarization produced by mechanical strains in crystals belonging to certain classes, the polarization being proportional to the strain and changing sign with it." Further discussion on piezoelectric effect and the constitutive relations is included later in the chapter.

Piezoelectricity occurs only in crystals which do not have a center of symmetry below Curie temperature. This study considers piezoelectric ceramics of Perovskite polycrystalline structures such as Barium Titanate, Lead Zirconate Titanate and other ceramics of the type ABO_3 (oxygen octahedral type unit cell), as shown in Fig. 1.

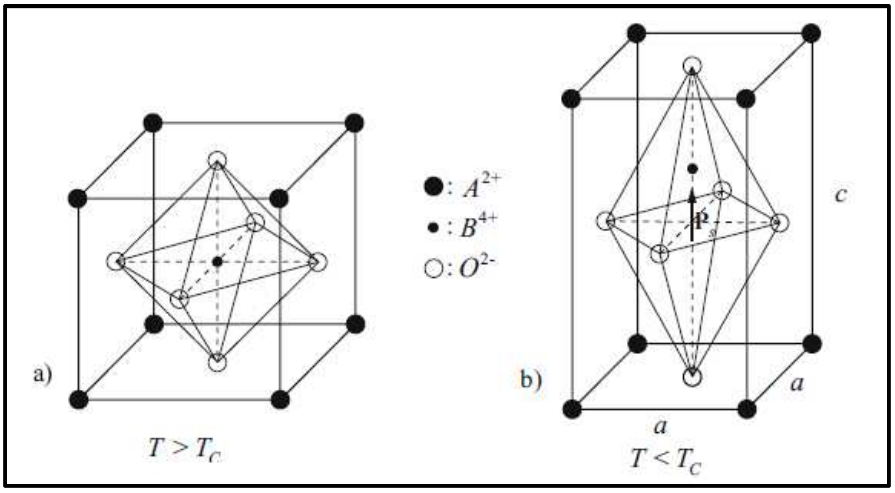

Figure 1: Perovskite structure of ferroelectric crystals of the type ABO_3 : (a) cube texture above Curie temperature; (b) tetragonal texture below Curie temperature[27]

Consider a Barium Titanate crystal above Curie temperature. It attains a cubic structure (see Fig. 1a) with Ba^{2+} at the corners, the O^{2-} at the face centers and Ti^{4+} at the center of the cube. This structure shows no piezoelectric properties. Below the Curie temperature, however, the crystal exists in the tetrahedral form where the ions are displaced relative to the earlier position. This shift creates an electric dipole and this is called spontaneous polarization which can occur in any of the six directions [28, 29].

We consider polycrystalline ceramics to be made up of grains and grain boundaries at a microstructural level. Based on the spontaneous polarization direction, the domains within a ferroelectric ceramic can be oriented differently in the different domains within the same grain. The net polarization for such a grain may be negligible at a global level and no notable piezoelectric effect (or inverse piezoelectric effect) can be seen under the

application of a mechanical or electrical stimulus. This ceramic can be poled in order to reorient the domains in a similar direction by the application of an electric field in the desired direction.

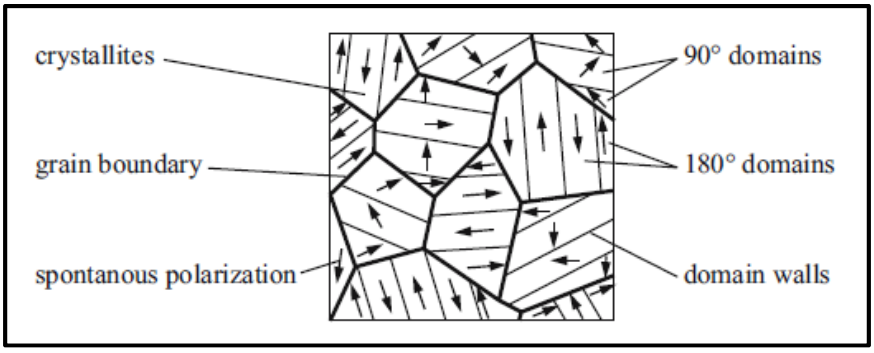

Figure 2: Polycrystalline ferroelectric crystal structure [27]

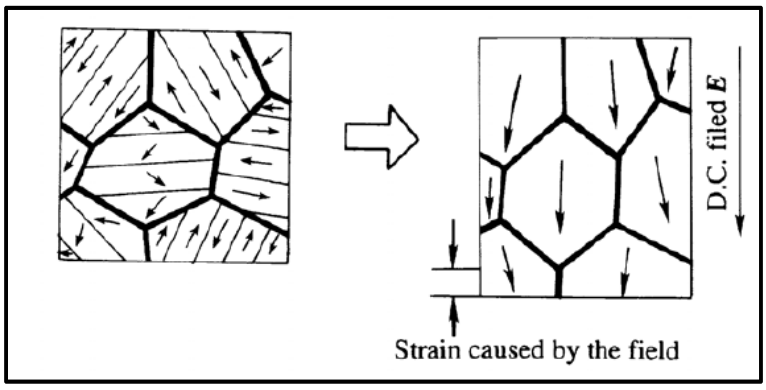

Figure 3: Domain orientation by poling (a) non polarized crystal; (b) polarized crystal [28]

Two kinds of domains are found to exist in such a ceramic: a 180º domain where adjacent regions have opposite polarization and 90º domains where adjacent regions

have perpendicular polarization (see Fig. 2). On the application of an electric field, the domains reorient themselves in the direction of the applied field (see Fig. 3). Switching of 180 º domains down not cause any strain but the switching of 90 º domains causes deformation in the ceramic on a macroscopic scale [29].

2.2 Electromechanical Coupling and Constitutive Equations

In a polarized ceramic, when the electric field E is applied parallel to the polarization direction, the remnant polarization is further aligned in the direction of the applied electric field. This causes elongation in the polarization direction (see Fig. 4). If the electric field were to be applied in the opposite direction to the poling direction, the domains would once again begin to switch to the new direction. In this case, the structure would contract along the polarization axis.

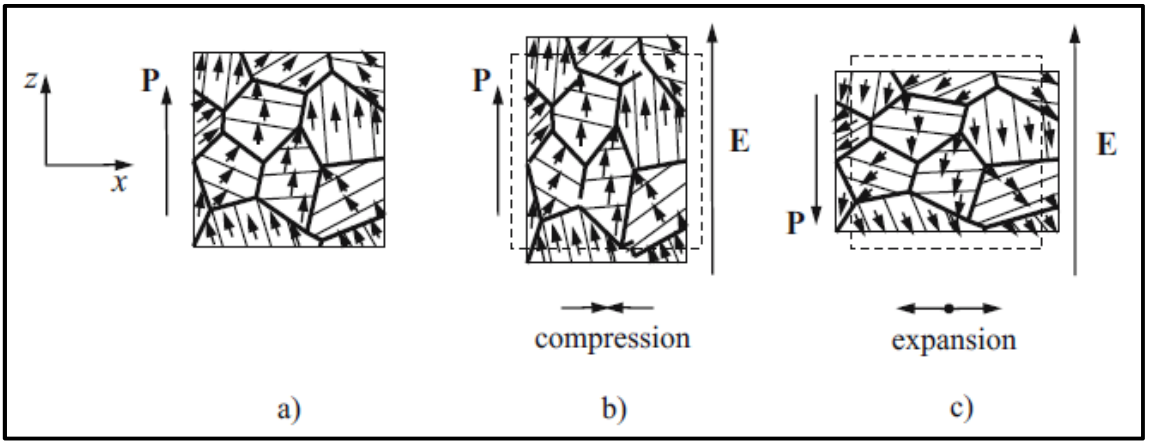

Figure 4: Transverse strain in ferroelectric ceramics: (a) Polarized state; (b) Electric field E parallel to polarization direction; (c) Electric field antiparallel to polarization direction [27]

As we know, if a stress is applied to an elastic material, there will be a corresponding strain in the material. At relatively low values of stresses, the corresponding strains are usually linearly proportional to the stresses. Now if a stress is applied to a poled piezoelectric material, the rotation of dipoles will cause collection of opposite charges on the electrodes. The electric displacement **D** (charge per unit area of electrode) is observed to be proportional to the applied stress at low values of stress. The constant of proportionality is called the piezoelectric strain coefficient.

Conversely, when an electric field **E** is applied across a piezoelectric material, the dipole rotation once again leads to an electric displacement **D** which is linearly proportional to the electric field. As per the inverse piezoelectric effect, this electric field also causes straining of the material. The strain is proportional to the electric field and, once again, the slope is the piezoelectric strain coefficient [30].

Considering the piezoelectric relations in all three directions, the constitutive relations foe linear electro-mechanical coupling response of polarized piezoelectric is written as:

$$\varepsilon_{ij} = s^{E}_{ijkl}\sigma_{kl} + d_{nij}E_n$$
$$D_m = d_{mkl}\sigma_{kl} + \grave{o}^{\sigma}_{mn}E_n \qquad \text{where i,j,k} = 1,2,3 \tag{2.1}$$

where ε is the strain, **σ** is the stress, d is the piezoelectric strain coefficient, **s** is the mechanical compliance, **D** is the electric displacement, **ϵ** is the dielectric permittivity and **E** is the electric field. These equations consider the stress and electric field as independent variables. An alternative expression is:

$$\sigma_{ij} = C_{ijkl}\varepsilon_{kl} + \mathrm{e}_{nij}E_n$$
$$D_m = \mathrm{e}_{mkl}\varepsilon_{kl} + \grave{\mathrm{o}}_{mn}E_n \qquad \text{where i,j,k} = 1,2,3 \tag{2.2}$$

where **e** is the piezoelectric stress coefficient and **C** is the stiffness. This set of equations considers the strain and the electric field as independent variables.

In Eq. 2.2, the stress and strain tensors have 9 elements each, the compliance and stiffness matrices have 81 constants each, the piezoelectric stress and strain coefficients have 27 constants and the permittivity matric is comprised of 9 values (see [31, 32]). Keeping in mind the symmetry conditions, the following engineering is quite common in literature and has been adopted here:

$$\begin{aligned}
&\sigma_1 = \sigma_{11} && \varepsilon_1 = \varepsilon_{11} \\
&\sigma_2 = \sigma_{22} && \varepsilon_2 = \varepsilon_{22} \\
&\sigma_3 = \sigma_{33} && \varepsilon_1 = \varepsilon_{33} \\
&\sigma_4 = \sigma_{23} = \sigma_{32} && \varepsilon_4 = \varepsilon_{23} + \varepsilon_{32} \\
&\sigma_5 = \sigma_{31} = \sigma_{13} && \varepsilon_5 = \varepsilon_{31} + \varepsilon_{13} \\
&\sigma_6 = \sigma_{12} = \sigma_{21} && \varepsilon_6 = \varepsilon_{12} + \varepsilon_{21}
\end{aligned} \tag{2.3}$$

This condenses the equations to:

$$\varepsilon_i = s_{ij}\sigma_j + d_{ni}E_n$$
$$D_m = d_{mj}\sigma_j + \grave{\mathrm{o}}_{mn}E_n \qquad \textit{where } i, j = 1,2,...6;\ m,n = 1,2,3 \tag{2.4}$$

$$\sigma_i = C_{ij}\varepsilon_j + \mathrm{e}_{ni}E_n$$
$$D_m = \mathrm{e}_{mj}\varepsilon_j + \grave{\mathrm{o}}_{mn}E_n \qquad \textit{where } i, j = 1,2,...6;\ m,n = 1,2,3 \tag{2.5}$$

Most polarized piezoelectric ceramics of Perovskit structures are orthotropic in nature. By making this assumption, the material constants in the above equation are as follows:

$$s = \begin{bmatrix} \frac{1}{Y_1} & -\frac{\nu_{12}}{Y_1} & -\frac{\nu_{13}}{Y_1} & 0 & 0 & 0 \\ -\frac{\nu_{21}}{Y_2} & \frac{1}{Y_2} & -\frac{\nu_{23}}{Y_2} & 0 & 0 & 0 \\ -\frac{\nu_{31}}{Y_3} & -\frac{\nu_{32}}{Y_3} & \frac{1}{Y_3} & 0 & 0 & 0 \\ 0 & 0 & 0 & \frac{1}{G_{23}} & 0 & 0 \\ 0 & 0 & 0 & 0 & \frac{1}{G_{23}} & 0 \\ 0 & 0 & 0 & 0 & 0 & \frac{1}{G_{23}} \end{bmatrix} \quad (2.6)$$

where $Y_i, \mathrm{i} = 1,2,3$ are the scalar components of the elastic Young's moduli in the 3 directions, ν_{ij} are the components of the Poisson's ratios and G_{ij} are the components of the shear moduli. The permittivity and piezoelectric constants with the non-zero components are written as:

$$\grave{o} = \begin{bmatrix} \grave{o}_{11} & 0 & 0 \\ 0 & \grave{o}_{22} & 0 \\ 0 & 0 & \grave{o}_{33} \end{bmatrix} \quad (2.7)$$

$$\mathbf{d} = \begin{bmatrix} 0 & 0 & 0 & 0 & d_{15} & 0 \\ 0 & 0 & 0 & d_{24} & 0 & 0 \\ d_{13} & d_{23} & d_{33} & 0 & 0 & 0 \end{bmatrix} \quad (2.8)$$

2.3 Operating Modes

There are two primary modes in which piezoelectric devices are commonly operated: the 33 and the 31 operating modes. Usually, the polarization direction is considered in the x_3 direction. The other two perpendicular directions are x_1 and x_2. In case of the 33 mode,

the stress, strain, electric displacement and electric field in the x_3-direction are considered in the applications. Thus, the d_{33} component of piezoelectric coefficient is utilized. By varying the mechanical load or displacement in the x_3-direction the electric charge D_3 can be collected and by prescribing an electric field E_3, changes in the displacement or force in the x_3-direction can be measured. In the 31 mode the deformations or forces of the structure in the x_1 and x_2 directions are obtained by prescribing an electric field along the poling direction x_3 and an electric charge D_3 can be collected due to changes in the displacements or forces in the x_1 and x_2 directions. When multiple piezoelectric wafers are stacked, with a common voltage across each of them a larger displacement can be achieved than by using a single actuator.

This study utilizes the 31 mode in order to induce bending on a piezoelectric functionally graded beam, in which the poling axis of the piezoelectric ceramics is in the through-thickness direction of the beam (x_3-axis) and the electric field E_3 is applied through the thickness of the beam. A non-uniform elongation or shortening in the axial (x_1-) direction of the piezoelectric components induces bending of the beam. Also, the Euler-Bernoulli beam model is considered for the piezoelectric functionally graded cantilever beam and the x_2-direction (y direction) is left out of the calculations. Thus, the constitutive equation for the piezoelectric beam reduces to:

$$\varepsilon_1 = \frac{1}{Y_1}\sigma_1 + d_{31}E_3$$
$$D_3 = d_{31}\sigma_1 + \grave{o}_{33}E_3 \qquad (2.9)$$

CHAPTER III

ELECTRO-THERMO-MECHANICAL BEAM BENDING FORMULATION

In this section the governing equations for beam bending in a piezoelectric functionally graded beam, which is approximated as layered piezoelectric composite beam, have been set up. All the symbols have been defined in the Nomenclature section at the beginning of this document. Here, we consider the problem of the beam bending in one plane only. The Euler-Bernoulli beam model is selected as a base thus the effects of transverse shear stresses on the lateral deflection have not been included in the study. The beam bending equations are set up for an *n*-layered beam. The approximation of a functionally graded beam to a multi-layer beam is discussed in Chapter IV.

Consider the displacement of point P after the deformation of a cantilever beam as shown in Fig. 5. The deformations of the cantilever are:

$$\begin{aligned} u_1 &= u_0 - z\theta \\ u_2 &= 0 \\ u_3 &= w \end{aligned} \tag{3.1}$$

where u_0 is the axial deformation of the neutral axis, z (or x_3) is the distance of any point in the beam from the neutral axis and θ is the rotation of the neutral axis. The mechanical strain components are given as follows:

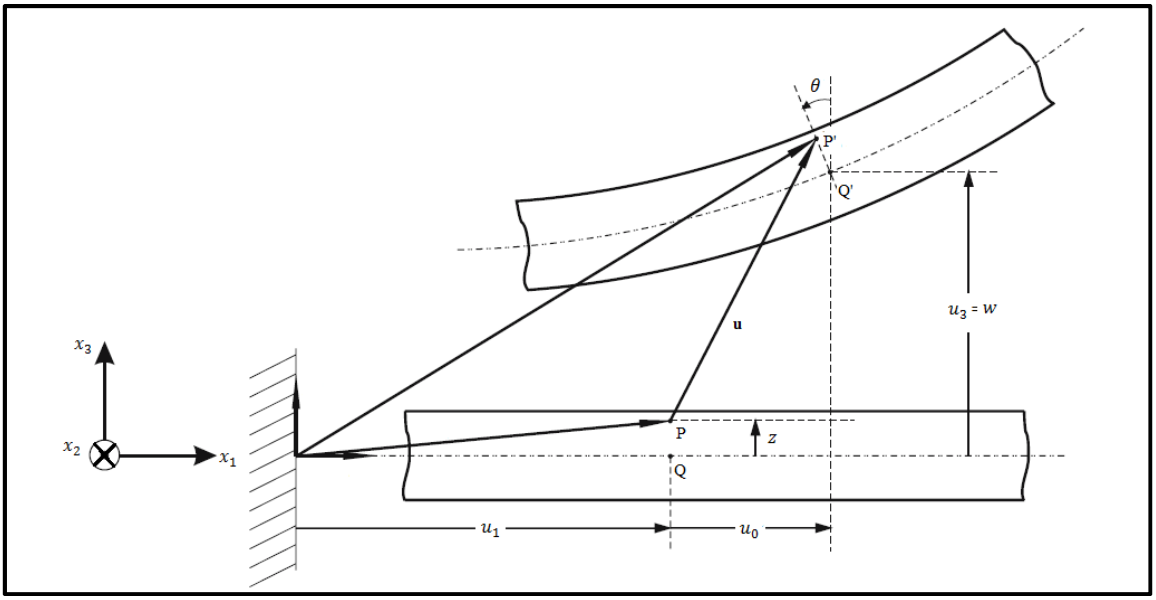

Figure 5: Elastic beam bending [27]

$$\varepsilon_{11} = \frac{\partial u_0}{\partial x_1} - z\frac{\partial \theta}{\partial x_1}$$
$$\varepsilon_{22} = 0 \tag{3.2}$$
$$2\varepsilon_{13} = \frac{\partial u_3}{\partial x_1} + \frac{\partial u_1}{\partial x_3} = \frac{\partial w}{\partial x_1} - \theta$$

As per the Euler-Bernoulli beam theory, there are no transverse strains i.e. $\varepsilon_{13} = 0$ and the rotational angle θ is defined as:

$$\theta = \frac{\partial w}{\partial x_1} \tag{3.3}$$

and the axial strain in Eq. (3.2), in engineering notation, becomes

$$\varepsilon_1 = \frac{\partial u_0}{\partial x_1} - z\frac{\partial^2 w}{\partial x_1^2} \tag{3.4}$$

For convenience, the above equation is expressed in terms of the axial strain at the neutral axis ε_0 and curvature K:

$$\varepsilon_0 = \frac{\partial u_0}{\partial x_1}; \qquad K = \frac{\partial^2 w}{\partial x_1^2} \tag{3.5}$$

Therefore,

$$\varepsilon_1 = \varepsilon_0 - zK \tag{3.6}$$

Further, the axial stress for a linear elastic beam is given by:

$$\sigma_1 = Y_1 \varepsilon_1 = Y_1(\varepsilon_0 - zK) \tag{3.7}$$

3.1 Thermo-elastic Strain

If a temperature change $T(z)$ is applied, the strain can be expressed as follows:

$$\varepsilon_1 = \varepsilon_0 - zK - \alpha_{11} T \tag{3.8}$$

where α_{11} is the coefficient of thermal expansion and T is the temperature change applied at a given point.

3.2 Piezo-thermo-elastic Strain

Incorporating the strain due to the piezoelectric and temperature effects in the above equation as per the discussion and equation 2.5 we obtain the following equation for the axial strain:

$$\varepsilon_1 = \varepsilon_0 - zK - \alpha_{11} T - d_{31} E_3 \tag{3.9}$$

Continuing with this expression for strain, the stress can be expressed as:

$$\sigma_1 = Y_1 \left(\varepsilon_0 - zK - \alpha_{11} T - d_{31} E_3 \right) \tag{3.10}$$

Here onward, the following symbols will be used for convenience:

σ for σ_1 for stress in x direction
ε for ε_1 for strain in x direction
Y for Y_1 for Young's Modulus in x direction
α for α_{11} for coefficient of thermal expansion in x direction
d for d_{31} for piezoelectric strain constant 31 component
E for E_3 for electric field in z direction
ò for $\grave{o}_{33}$ for dielectric constant 33 component

3.3 Locating the Neutral Axis

Let $\bar{z}$ be the distance of the neutral axis from the bottom edge of the beam. In order to locate the neutral axis, we assume a case of pure bending i.e. $\varepsilon_0 = 0$

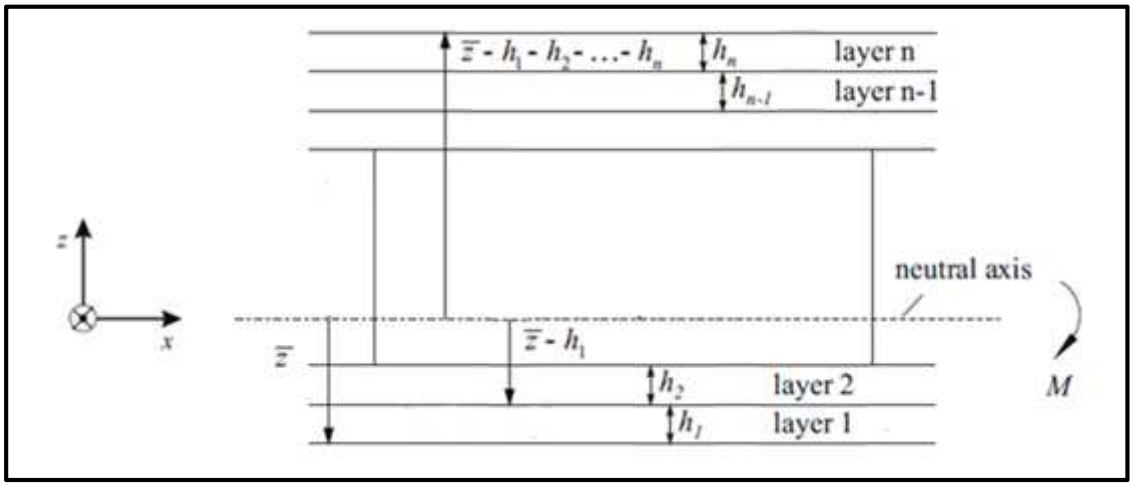

Figure 6: *n*-layered beam [27]

In order to find the neutral axis, we sum forces in the x-direction i.e. $\sum F_1 = 0$. Therefore,

$$\int_A \sigma dA = 0 \tag{3.11}$$

Substituting the expression for stress from Eq. 3.7,

$$\int_A Y(-zK)dA = 0 \tag{3.12}$$

For the multilayered beam considered in this problem (see Fig. 6), we assume the material properties to be constant over each layer. So the expression in Eq. 3.12 is applied to each layer and the results over all the layers are summed. This is the expression for stress over any layer i.

$$\sigma^i = Y^i\left(\varepsilon_0 - zK\right) \tag{3.13}$$

$$\sum_{i=1}^{n} \int_{A_i} Y^i (zK) dA_i = 0 \tag{3.14}$$

$$\sum_{i=1}^{n} b^i \int_{z_{i-1}}^{z_i} Y^i zK dz = 0 \tag{3.15}$$

$$\sum_{i=1}^{n} \frac{b^i Y^i K}{2}\left(z_i^2 - z_{i-1}^2\right) = 0 \tag{3.16}$$

where z_i and $z_{i-1}$are the upper and lower limits respectively of the i^{th} layer of the beam.

$$z_{i-1} = -\left(\bar{z} - \sum_{j=1}^{i-1} h_j\right) \quad \text{and} \quad z_i = -\left(\bar{z} - \sum_{j=1}^{i} h_j\right) \tag{3.17}$$

Substituting these values in Eq. 3.12, and solving for $\bar{z}$:

$$\sum_{i=1}^{n}\frac{b^iY^iK}{2}\left[\left(\bar{z}-\sum_{j=1}^{i}h_j\right)^2-\left(\bar{z}-\sum_{j=1}^{i-1}h_j\right)^2\right]=0$$

$$\sum_{i=1}^{n}\frac{b^iY^iK}{2}\left[\left(\bar{z}-\sum_{j=1}^{i}h_j\right)^2-\left(\bar{z}-\sum_{j=1}^{i}h_j+h_i\right)^2\right]=0$$

$$\sum_{i=1}^{n}b^iY^i\left[\left(\bar{z}-\sum_{j=1}^{i}h_j\right)^2-\left(\bar{z}-\sum_{j=1}^{i}h_j\right)^2-h_i^2-2h_i\left(\bar{z}-\sum_{j=1}^{i}h_j\right)\right]=0$$

$$\sum_{i=1}^{n}b^iY^i\left[2h_i\sum_{j=1}^{i}h_j-h_i^2-2h_i\bar{z}\right]=0 \tag{3.18}$$

$$\bar{z}=\frac{2\sum_{i=1}^{n}b^iY^ih_i\sum_{j=1}^{i}h_j-\sum_{i=1}^{n}b^iY^ih_i^2}{2\sum_{i=1}^{n}b^iY^ih_i} \tag{3.19}$$

3.4 Setting-up the Equations

Continuing from Equation 3.10, the piezo-thermo-elastic stress in the i^{th} layer is:

$$\sigma^i=Y^i\left(\varepsilon_0-zK-\alpha^iT^i-d^iE\right) \tag{3.20}$$

If the external axial force and bending moment applied are $N=\mathrm{N}_1$ and $\mathrm{M}=\mathrm{M}_2$ respectively, summing the forces and moments, we get:

From $\sum F_1 = 0$:

$$\sum_{i=1}^{n} b^i \int_{z_{i-1}}^{z_i} Y^i \left(\varepsilon_0 - zK - \alpha^i T^i - d^i E\right) dz = N \tag{3.21}$$

$$\begin{aligned} &\sum_{i=1}^{n} b^i Y^i \varepsilon_0 \left(z_i - z_{i-1}\right) - \sum_{i=1}^{n} \frac{b^i Y^i K}{2} \left(z_i^2 - z_{i-1}^2\right) \\ &- \sum_{i=1}^{n} b^i Y^i \alpha^i T^i \left(z_i - z_{i-1}\right) - \sum_{i=1}^{n} b^i Y^i d^i E \left(z_i - z_{i-1}\right) = N \end{aligned} \tag{3.22}$$

Therefore,

$$A\varepsilon_0 - BK = N + N^T + N^E \tag{3.23}$$

where

$$\begin{aligned} A &= \sum_{i=1}^{n} b^i Y^i \left(z_i - z_{i-1}\right) \\ B &= \sum_{i=1}^{n} \frac{b^i Y^i}{2} \left(z_i^2 - z_{i-1}^2\right) \\ N^T &= \sum_{i=1}^{n} b^i Y^i \alpha^i T^i \left(z_i - z_{i-1}\right) \\ N^E &= \sum_{i=1}^{n} b^i Y^i d^i E \left(z_i - z_{i-1}\right) \end{aligned} \tag{3.24}$$

From $\sum M = 0$:

$$\sum_{i=1}^{n} b^i \int_{z_{i-1}}^{z_i} Y^i K \left(\varepsilon_0 - zK - \alpha^i T^i - d^i E\right) z dz = M \tag{3.25}$$

$$\begin{aligned} &\sum_{i=1}^{n} \frac{b^i Y^i \varepsilon_0}{2} \left(z_i^2 - z_{i-1}^2\right) - \sum_{i=1}^{n} \frac{b^i Y^i K}{3} \left(z_i^3 - z_{i-1}^3\right) \\ &- \sum_{i=1}^{n} \frac{b^i Y^i \alpha^i T^i}{2} \left(z_i^2 - z_{i-1}^2\right) - \sum_{i=1}^{n} \frac{b^i Y^i d^i E}{2} \left(z_i^2 - z_{i-1}^2\right) = M \end{aligned} \tag{3.26}$$

So,

$$B\varepsilon_0 - DK = M + M^T + M^E \tag{3.27}$$

where

$$\begin{aligned} B &= \sum_{i=1}^{n} \frac{b^i Y^i}{2}\left(z_i^2 - z_{i-1}^2\right) \\ D &= \sum_{i=1}^{n} \frac{b^i Y^i}{3}\left(z_i^3 - z_{i-1}^3\right) \\ M^T &= \sum_{i=1}^{n} \frac{b^i Y^i \alpha^i T^i}{2}\left(z_i^2 - z_{i-1}^2\right) \\ M^E &= \sum_{i=1}^{n} \frac{b^i Y^i d^i E}{2}\left(z_i^2 - z_{i-1}^2\right) \end{aligned} \tag{3.28}$$

Knowing all the material constants, the Equations 3.20 and 3.24 can be solved to find the axial strain ε_0 and curvature K:

$$\begin{bmatrix} A & B \\ B & D \end{bmatrix} \begin{Bmatrix} \varepsilon_0 \\ -K \end{Bmatrix} = \begin{Bmatrix} N + N^T + N^T \\ M + M^T + M^E \end{Bmatrix} \tag{3.29}$$

Note that N, the external axial force is assumed to have been applied at the neutral axis. However, if this force is applied eccentrically, a corresponding moment must be assumed to compensate for the eccentricity.

Further, the x_1- and x_3- components of displacement i.e. u_1 and u_3 respectively can be calculated by knowing ε_0 and curvature K and from on Equations 3.1 and 3.5.

CHAPTER IV

RESPONSES OF A PIEZOELECTRIC FUNCTIONALLY GRADED BEAM: PARAMETRIC STUDIES

4.1 Problem Modeling

4.1.1 Materials Used

For this study, the metal selected is Titanium Alloy (Ti6AlV) and the piezoelectric ceramic is PZT 5A. The material data are provided below in Tables 1 and 2. The temperature dependent properties of PZT5A (piezoelectric strain constant d_{31}, coefficient of relative permittivity and coefficient of thermal expansion) are obtained through the data provided in [33, 34]. The temperature-dependent properties are given in Figs. 7-9.

Table 1: Material properties for elastic material Ti6AlV [35]

Elastic Material: Titanium alloy - Ti6AlV				
Property	Symbol	Units	Constant Value	Temperature-Dependent Value
Density	P	kg/m^3	4429	NA
Conductivity	K	W/m.K	6.7	=1.20947+168.569E-4**T**
Coefficient of Thermal Expansion	A	/K	8.6	=7.57876E-6 + 4.926E-9**T** + 2.3848E-12 $\mathbf{T^2}$
Poisson's Ratio	N	-	0.3	NA
Specific Heat Capacity	Cv	J/kg.K	526.3	=625.29692 - 0.2641**T** + 4.4888E-4 $\mathbf{T^2}$
Young's Modulus	E	N/m^2	1.13E+11	=122.55676E9 - 56.208E6 $\mathbf{T^2}$ - 45.12$\mathbf{T^3}$
Relative Permittivity	Er	-	1	NA
Piezoelectric Strain Constants	d31	C/N	0.00	NA
	d15	C/N	0.00	NA
	d33	C/N	0.00	NA

Table 2: Material properties for PZT 5A [34]

Piezoelectric Material: PZT 5A				
Property	Symbol	Units	Constant Value	Temperature-Dependent Value
Density	P	kg/m^3	7750	NA
Conductivity	K	W/mC	1.25	NA
Coefficient of Thermal Expansion	A	/K	3.00E-06	= 1.0014E-6 + 4.6429E-9**T** + 7.4286E-11 $\mathbf{T^2}$ – 2E-13 $\mathbf{T^3}$
Poisson's Ratio	N	-	0.31	NA
Specific Heat Capacity	Cv	J/kg.C	420	NA
Young's Modulus	E	N/m^2	1.21E+11	NA
Relative Permittivity	Er	-	-1700	= 1612.6 + 7.2619T -0.017405T2 + 7.6237E-5T3
Piezoelectric Strain Constants	d31	C/N	-1.71E-10	= -1.464E-10 - 5.2506E-13 **T** + 2.5515E-15 $\mathbf{T^2}$ - 4.3906E-18$\mathbf{T^3}$
	d15	C/N	5.84E-10	NA
	d33	C/N	3.74E-10	NA

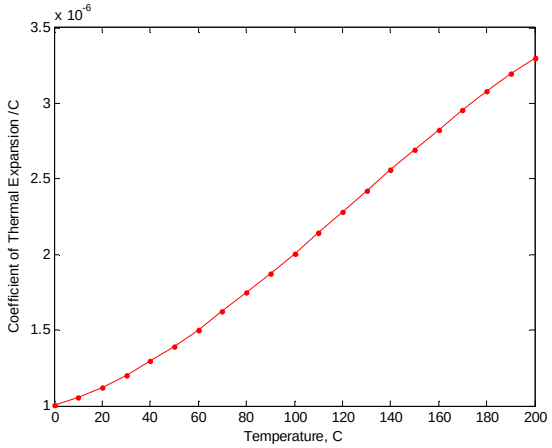

Figure 7: Coefficient of thermal expansion

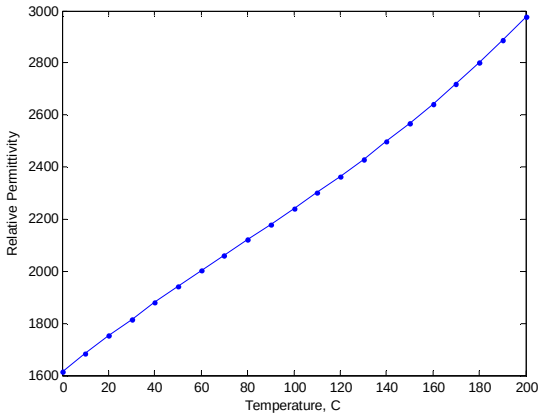

Figure 8: Relative permittivity

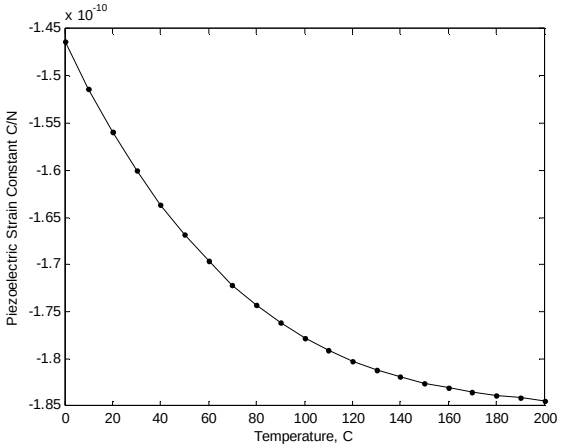

Figure 9: Piezoelectric strain constant

4.1.2 Functional Grading

The beam considered for this study is assumed to be a functionally graded composite beam in which the metal and ceramic constituents have been gradually varied from one end to another (see Fig. 10) through the thickness of the beam.

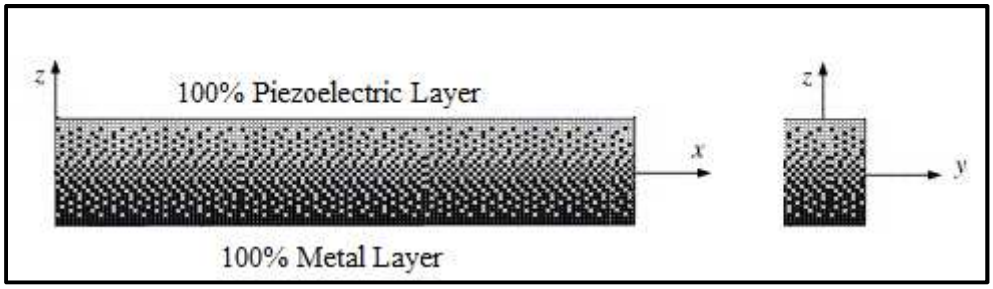

Figure 10: Functionally graded beam

The variation of the material through the thickness is assumed to follow a simple power law equation [23]:

$$P(z,T) = [P_c(T) - P_m(T)]\, f(z) + P_m(T) \tag{4.1}$$

$$f(z) = \left(\frac{1}{2} + \frac{z}{h}\right)^n \tag{4.2}$$

where n is the power law exponent, z is the perpendicular distance of any point in the beam from the center of the beam and T is the temperature of the material at that point. $f(z)$ is the volume fraction and $P(z,T)$ is any property of the material (e.g. coefficient of thermal expansion, Poisson's ratio etc.). P_c and P_m are the values of that property for the ceramic and metal respectively. In the case where the properties are independent of temperature, the above equation is dependent only on the through thickness location z.

In this study, it is assumed that the functionally graded beam is made up of discrete layers and that the material properties do not vary through a single layer. Since the material properties are graded gradually, the value of a material property will not vary greatly from one layer to the next. Each layer will thus have different material properties and the formulation for such an *n*-layered beam has been developed in Chapter III.

4.2 Results

A cantilever beam of 120mm length and 6mm x 6mm cross section is assumed for this study, making the *L/B* ratio 20. The initial temperature T_0 of the system is assumed to be 25C (see Fig. 11). The metal surface is maintained at this temperature for all parametric studies. The electric field *E* is applied through the thickness of the beam. In order to do this, electrodes are applied at the metal and PZT layers. For solving this beam bending problem, the heat transfer analysis is carried out first. The electric field and concentrated moment (electric and mechanical load cases) are assumed to act after the steady state had been reached.

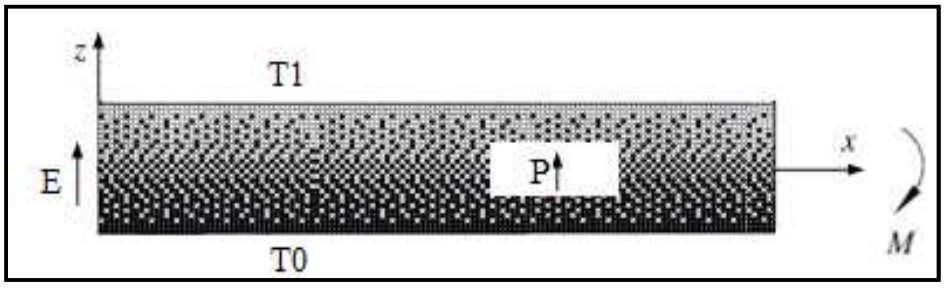

Figure 11: Problem description

4.2.1 Applying Electric Field Only

The coercive electric field magnitude for PZT 5A is 1200 V/mm. Therefore, the maximum field strength applied in this study has been restricted to 1000V/mm. The first case study is to examine the effect of gradual variation in the material properties, through varying the parameter n in Eq. (4.2), on the overall tip deflection at the free end of the cantilever beam. As the magnitude of the electric field applied increases, for any given value of n, the tip displacement monotonically increases (see Fig. 12). The through-thickness axial strain profiles at the maximum electric field (1000V/mm) are shown in Fig. 13. The application of the through-thickness electric field induces pure bending deformation in the functionally graded beam. It is evident that the strain is less than 2% and thus in keeping with the small strain assumption. The above study considers a functionally graded beam comprising of 6 layers.

Next, the effect of number of discrete layers n on the overall response of the functionally graded beam is studied. The variation of the lateral displacement with the number of layers is shown in Fig. 14 and serves as a convergence study. For 10 layers or more, the difference in the response is less than 1% so 10 or more layers may be used for the computation. However, in the event of manufacturing a beam of similar dimensions, 6 layers provide a fairly reasonable estimate of the response. The 6-layer response differs from the 10-layer response by about 2% for the n=1 case.

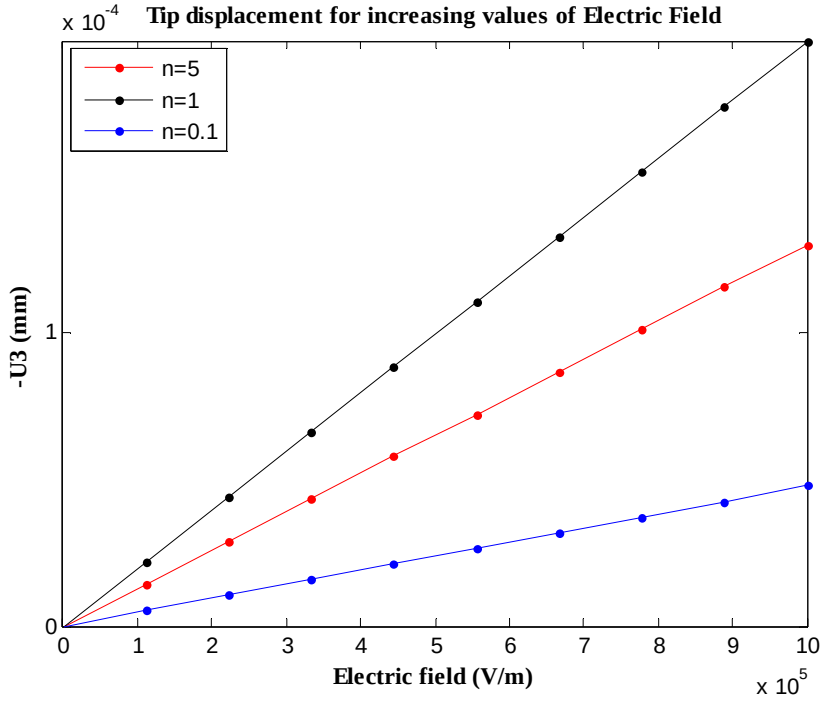

Figure 12: Variation of lateral deflection with electric field

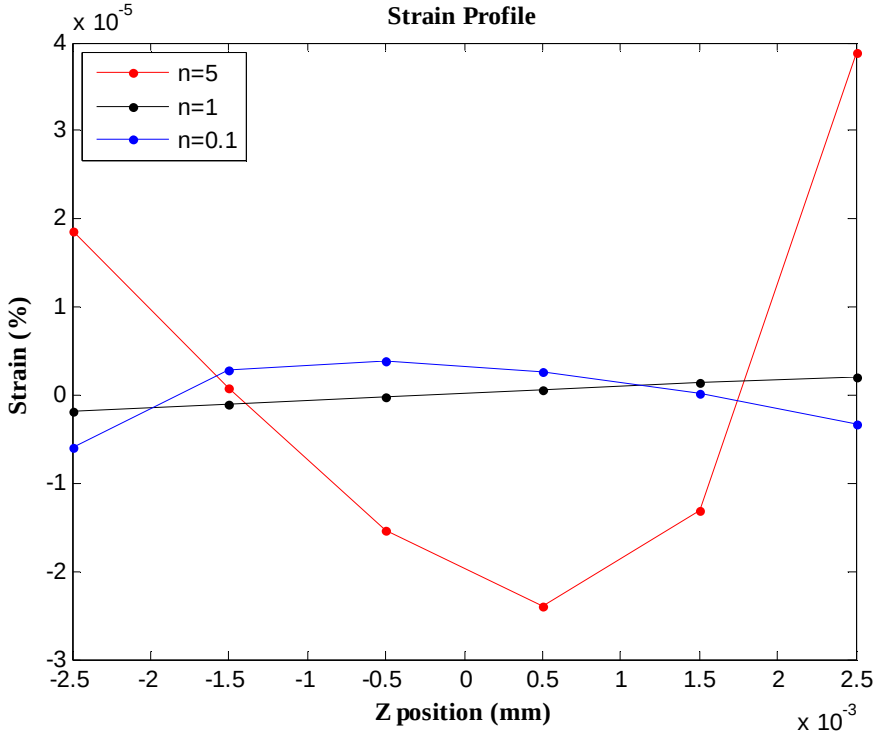

Figure 13: Strain profile for electric field of 1000V/mm

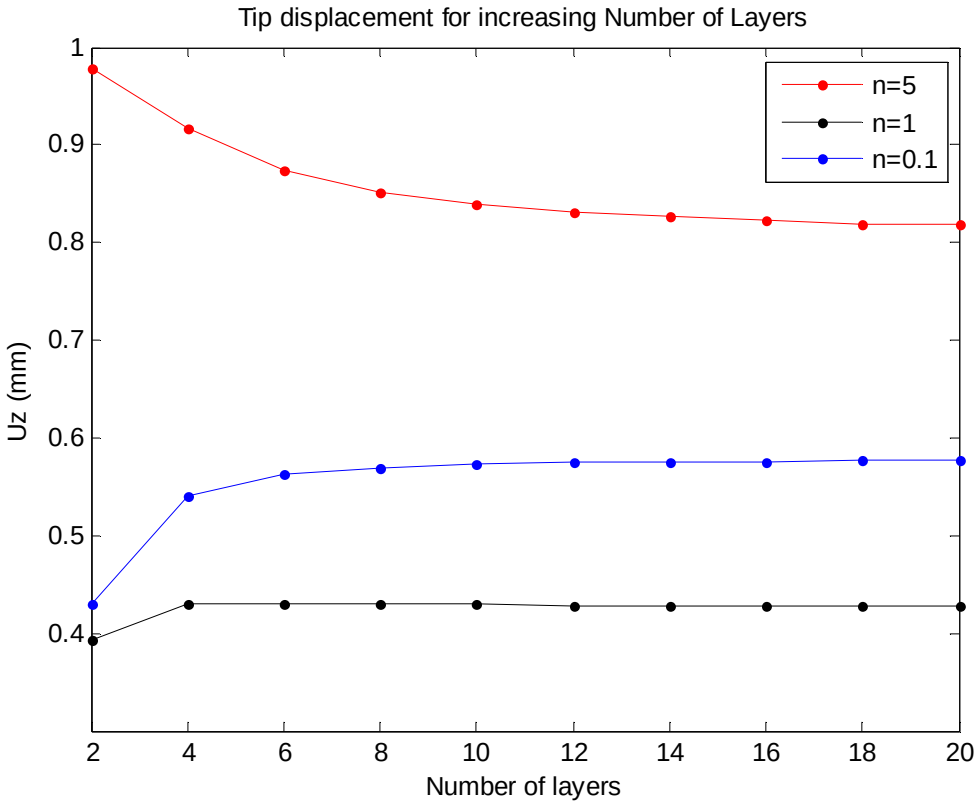

Figure 14: Variation of displacement response with the number of layers assumed for computation.

4.2.2 Applying Electric and Temperature Field

Here the piezoelectric layer was subjected to a temperature of T_1 on the ceramic layer (see Fig. 11). The Curie temperature in PZT 5A samples from various manufacturers has been recorded as being higher than 200^{o}C. Here, however, the maximum temperature has been restricted to 200^{o}C. This study considers a functionally graded beam comprising of 6 layers.

Consider the variation of the lateral deflection with respect to changing the gradation exponent n. A temperature T_1 =200C was applied at the PZT surface. This temperature change causes deflection in the beam. In order to minimize the tip deflection due to the temperature changes, electric field was applied in the direction of the polarization. Three values of electric field were considered: 0, 500 and 1000 V/mm. The lateral deflection in each case has been shown in Fig. 15. The lateral deflection hits a minimum value between 0 and 1. The minimum value is 0.6mm for E = 0, 0.52mm at n = 0.35, 0.52mm for E = 500V/mm at n = 0.7 and 0.43mm for E = 1000V/mm and n = 0.85. Thus, the graph indicates that as the electric field increases, the deflection is minimized to a greater extent and the minimum shifts to the right and its magnitude decreases. This is obvious, since the electric field counters the deflection due to the thermal load. Hence, the total deflection in the beam is minimized as the electric field increases. The same trend is also observed in all load cases. If the external loads are known for a given application, it would be possible to select an optimal *n*-value to minimize the lateral deflection in the beam.

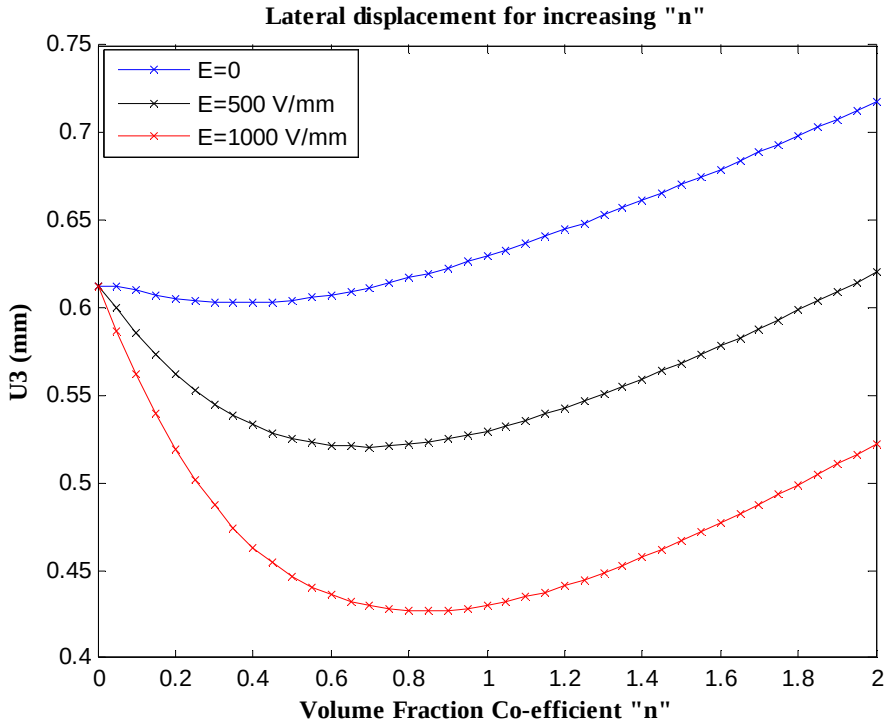

Figure 15: Lateral deflection with respect to coefficient n (E = 1E6V/m)

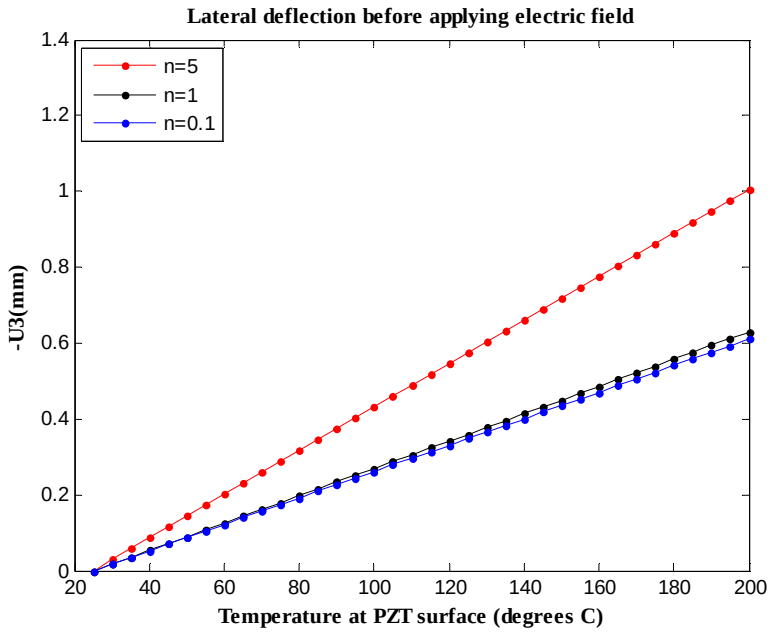

Figure 16: Lateral displacement as a function of the temperature at PZT surface

A temperature field is created by applying a temperature T_1 at the piezoelectric surface and Fig 16 shows the variation of the lateral displacement with T_1. For this, T_1 was varied from 25C to 200C. The deflection due to the applied thermal field is downward and hence negative. The –U3 value has been plotted the graph shown. The maximum displacement (occurring for T_1 = 200C) is ~0.6mm for both n=1 and n=0.1 and 1mm for n=5. The lateral displacement steadily increases with an increase in temperature since the material properties here are assumed to be independent of temperature.

With an intention to minimize the deflection of the free end of the cantilever actuator, the next step is to find the electric field required in order to mitigate the bending due to the applied temperature field. Figure 17 shows the variation in electric field strength required for an increasing value of T_1 (i.e. the temperature applied at the piezoelectric surface). This value directly depends upon the deflection shown in Fig. 16 and hence, this too, varies linearly with the temperature applied. The electric field required for minimizing the displacement due to temperature is 14000V/mm for n=0.1, 8000V/mm for n=5 and 3000V/mm for n=1. Since the piezoelectric constituent is the least in case of n=0.1, even though it has lower displacement than n=5, the electric field required to negate that displacement is higher for n=0.1. Obviously, since the coercive field is 1200V/mm, the demand of 14000V/mm cannot be met and is not a realistic value. However, a field of 1000V/mm was applied to note the reduction in displacement that can be achieved.

Fig. 18 shows the reduction in lateral displacement after the electric field has been applied to a thermal load case for linear material grading. While the deflection is reduced by almost 30% in this case (n=1), the magnitude of this difference is about 0.2mm. It is important to note that this mitigation in displacement depends solely upon the electric field applied and this is a reasonably large percentage of the initial displacement for n values close to 1. However, for larger displacements such as for a large n value, it may not be a significant percentage of the initial deflection.

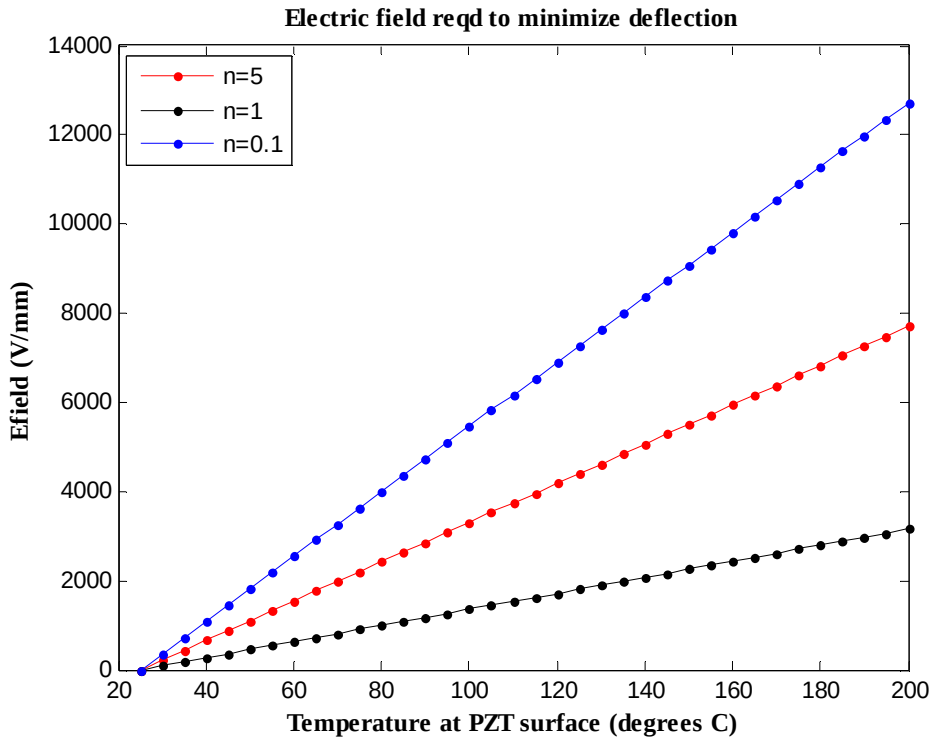

Figure 17: Electric field strength required to minimize the lateral displacement due to the thermal field applied

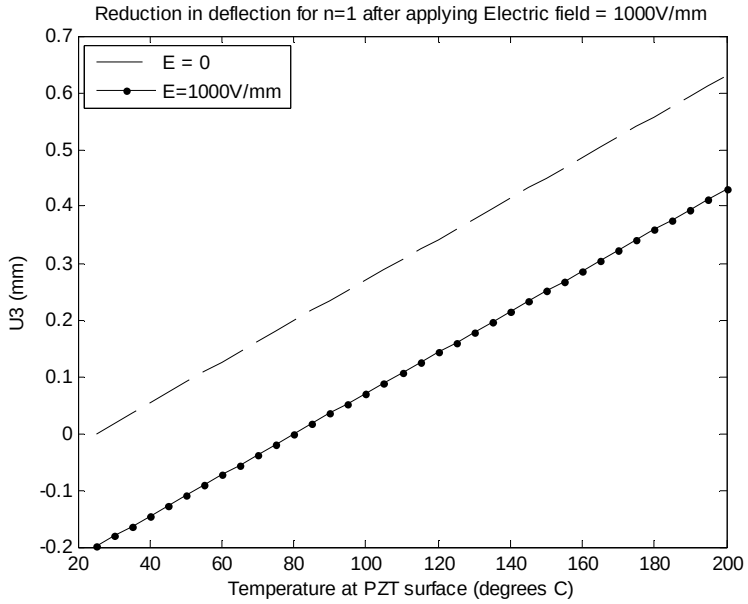

Figure 18: Change in lateral displacement on applying electric field

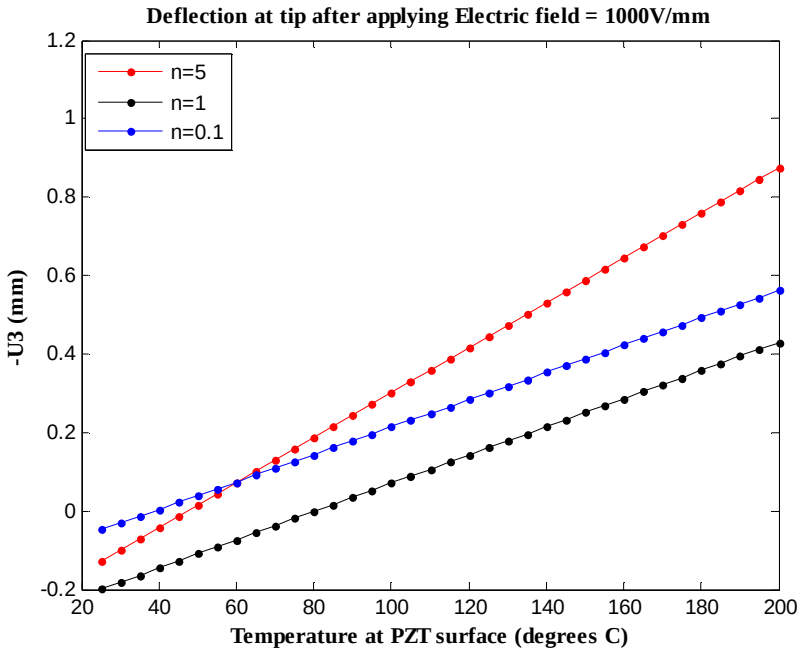

Figure 19: Deflection after applying electric field

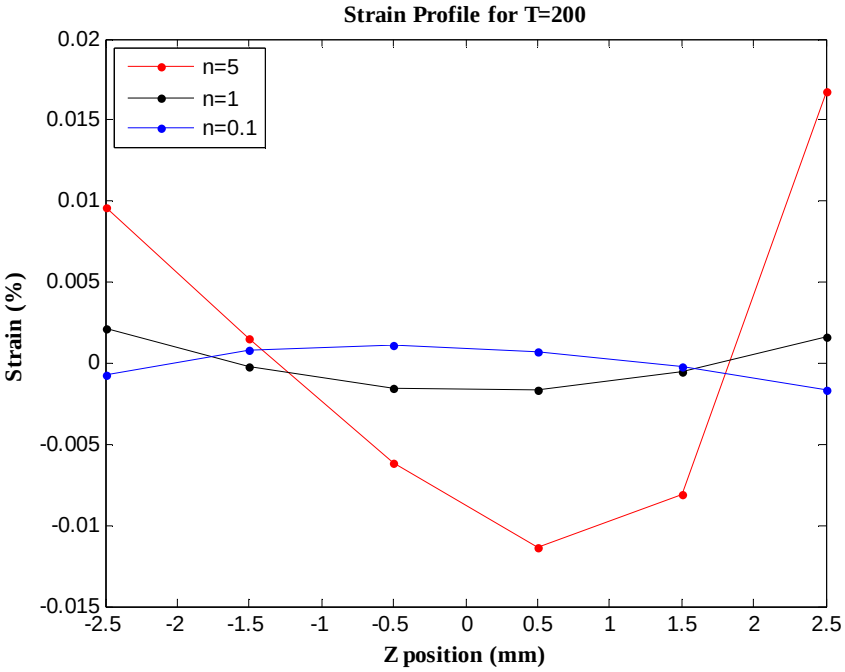

Figure 20: Strain profile for electrical + thermal load case

Figure 19 shows the deflection observed after the electric field has been applied. Even though initially the deflection values were very close for both n=1 and n=0.1, it can be seen that the deflection is reduced to a greater extend for the n=1 beam. The maximum value for n=1 is reduced from 0.63mm to 0.43mm, for n=0.1 from 0.61mm to 0.56mm and for n=5 from 1mm to 0.87mm. This difference is due to the varying piezoelectric effect seen in the beams.

It can be observed from Fig. 20 that for a lower n-value the strain profile predicted is smoother than for larger n-values. For an n=5 value, the material properties change more rapidly closer to the PZT surface. Thus assuming layers of equal size is not the most accurate basis for predicting the response of the beam. Similarly, the properties vary

rapidly closer to the metal surface for n values less than 1. It will be more advantageous to assume layers of unequal thickness. For example, for n=5, it would be useful to assume thicker layers close to the metal surface and thinner layers close to the ceramic surface. This would predict a smoother strain response for the beam as would be expected in a functionally graded material.

Now the same problem is solved for a case where certain material properties vary with the temperature. The thermal conductivity varies with temperature in case of the Titanium alloy while the conductivity is a constant value for the PZT. The electric field required is shown in Fig. 21.It is observed that the electric field required to minimize the deflection is 7200V/mm for n=5, 2700V/mm for n=1 and 8300 V/mm for n=0.1.

Fig. 22 compares the deflection in both cases (temperature dependent and independent) after the electric field has been applied. The response predicted by the temperature-dependent model is slightly lower than that predicted by the temperature independent model. Also, it is noticed that the difference is more pronounced towards the middle of the temperature change i.e. close to 100C.

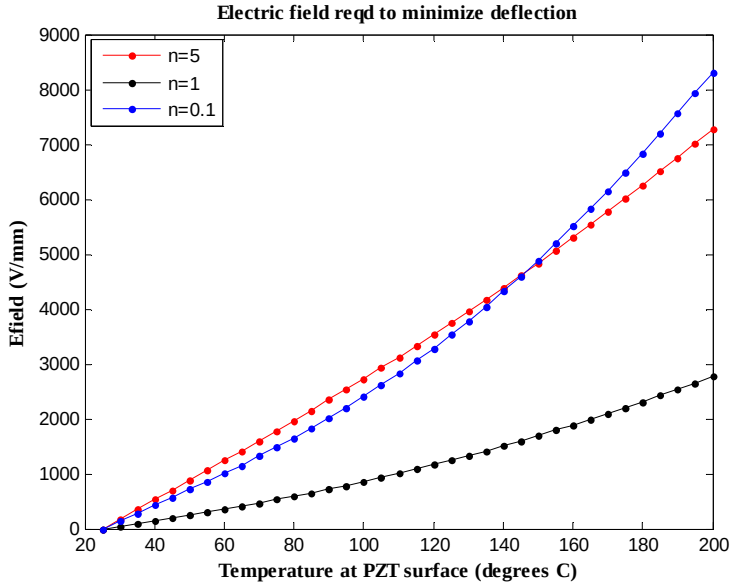

Figure 21: Electric field required to minimize displacement by the temperature-dependent model.

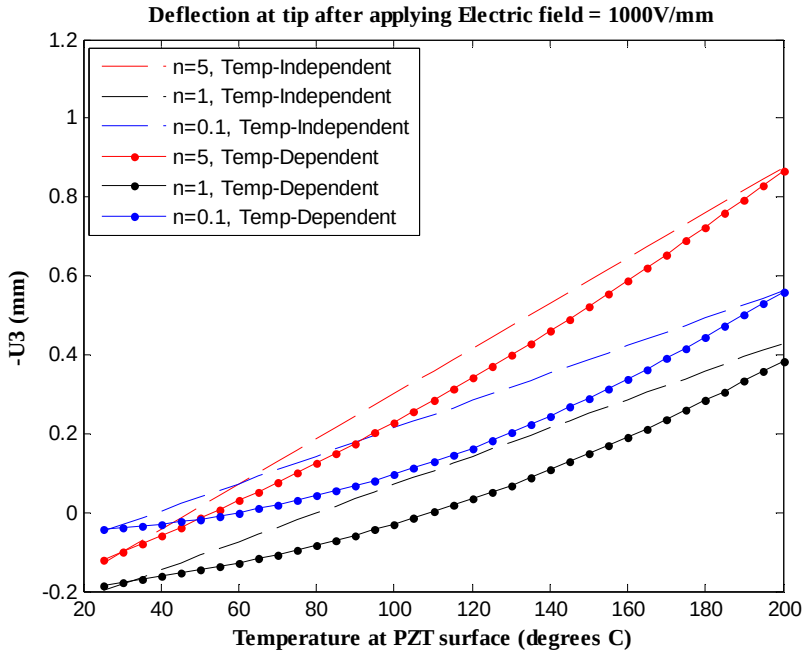

Figure 22: Comparison of deflection predicted by temperature dependent and independent models

4.2.3 Applying Mechanical, Thermal and Electrical Load

In addition to the above loads, a mechanical loading is considered here. T_1 is taken as 200C for all problems. A moment M is applied at the free end of the cantilever and its value ranges from -0.5Nm to 0.5Nm. The electric field required to minimize the deflection for both the temperature-dependent and independent cases have been shown in Fig. 23. As seen in the earlier case, the electric field strength required is much higher for n = 0.1 than for the other two cases due the lower piezoelectric effect. In case of n=0.1, the difference between the temperature dependent and independent models is also larger. On the other hand, this difference is quite small for n=1 and n=5. The maximum electric field is required for the +0.5Nm moment the maximum difference for the two models is 35% for n=0.1, 12% for n=1 and 14% for n=5.

The corresponding displacement after applying the electric field of strength 1000V/mm can be seen in Fig 24. The dashed line signifies the temperature-dependent model and the dotted line signifies the temperature-independent model. The maximum difference between the two models is seen for n=1 followed by n=5 and the least is for n=0.1. The least displacement of all is seen in the n=1 case – only about 0.65mm. The strain profiles for the extreme moment cases have been shown in Fig. 25 (after the electric field has been applied for the n=1 case). It can be observed that the strain profiles show a slightly smaller value in case of the temperature-dependent model. As the n=1 case has the smallest displacement, it also shows very small values (less than 0.015%) of strain once the deflection has been minimized by applying an electric field.

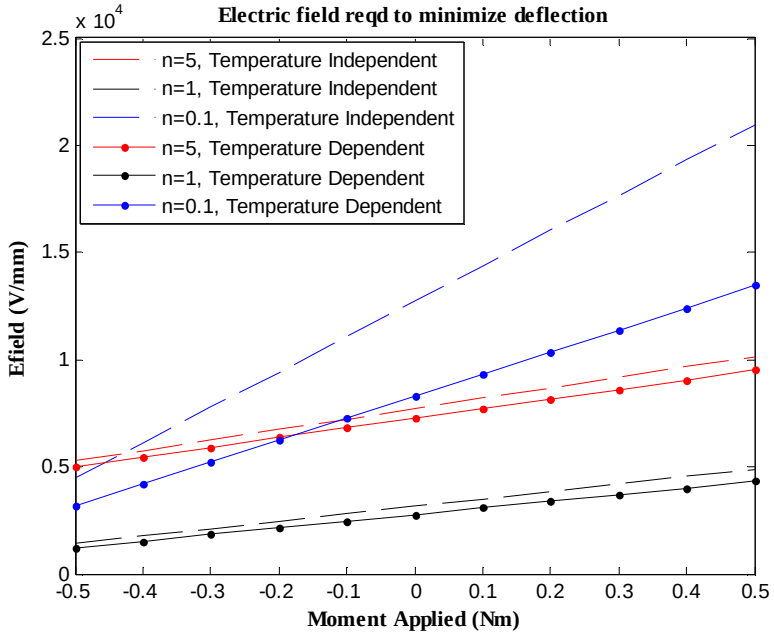

Figure 23: Comparison of electric field strength required in order the minimize tip deflection

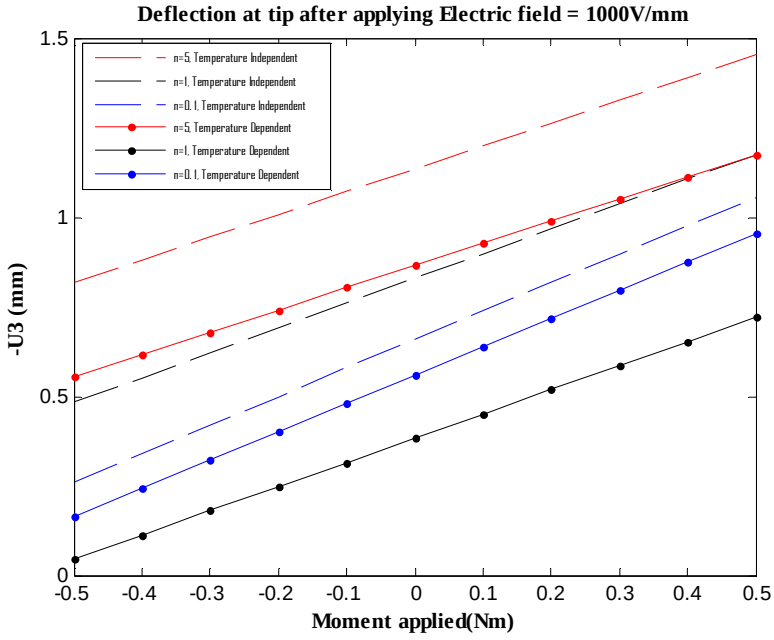

Figure 24: Comparison of the lateral displacement as a function of the concentrated moment applied

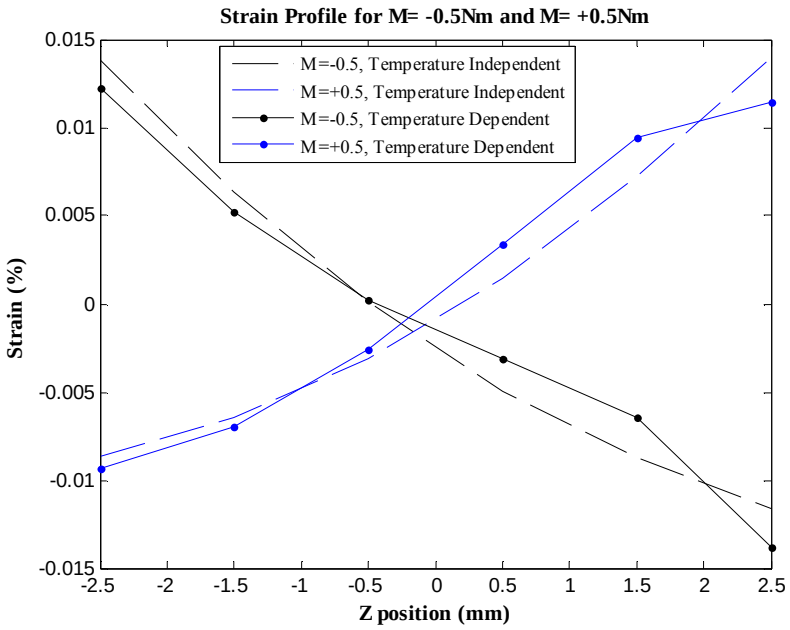

Figure 25: Strain profile for temperature dependent case (solid, marked line) and temperature independent (dashed line) case.

CHAPTER IV

CONCLUSIONS AND DISCUSSION

5.1 Conclusions

In this study, a functionally graded composite having discrete layers of piezoelectric ceramic/metal composite is analyzed based on a multi-layer Euler-Bernoulli beam model. The governing equation for such a piezoelectric functionally composite beam is developed and the overall displacement response of the beam under thermal, mechanical and electrical stimuli is predicted. The analysis is performed in two steps: (a) finding the temperature profile from the heat transfer analysis and (b) finding the displacement response from the beam bending analysis. Further, two models have been considered: one with temperature-independent material properties and another with temperature dependent material properties.

In order to approximate the functionally graded beam to a multi-layered model, *n* equal layers are assumed. The functionally graded properties for the center of each layer are found based on rule of mixture and they are assumed to be constant for that layer. A temperature field is created by applying a fixed temperature at the extreme metal and ceramic surfaces. It is assumed the beam reaches a thermal steady state before the application of mechanical and electrical inputs. The mechanical load is in the form of a concentrated moment at the free end of the cantilever beam. Electric field was supplied

in order to minimize the deflection caused by thermal and mechanical load. Since the dimensions were reasonably small, it was assumed that the electrodes were placed along the top and bottom faces of the beam thus giving an even field strength throughout the beam. The limiting factor for minimizing deflection in this manner is the coercive field limit. In fact, in reality, as the electric field gets very close to the coercive field value, the material behaves non-linearly. This factor has not been discussed in this study. It would also be possible to provide multiple electrodes through the thickness. Doing so makes it possible to provide differential electric field through different layers of the beam. This behavior can be used to further control the deflection in the beam.

The main purpose of incorporating a functionally graded type material in actuators is to reduce the stress concentration at the layer interfaces. It is observed that the strain and corresponding stress in the beam is fairly smooth due to the gradual variations on the properties of the beam. This can help avoiding debonding between layers that occurs in laminated composites.

Obviously, incorporating a temperature-dependent model is a more realistic prediction of the beam bending response. Based on the material properties assumed, the deflection predicted by the temperature-dependent model is slightly lower than that predicted by the temperature-independent model. However, within the limitations of the coercive field and Curie temperature, the two values are not widely different. There has been some research in the past on high-temperature piezoelectric materials. Incorporating

such a ceramic would allow a wider range of applied temperatures and it is likely that the temperature effects would be more significant. Metal ceramic functionally graded composites are already being used as thermal barriers. Developing a similar metal-PZT composite would provide an ideal transducer in high temperature fields.

5.2 Limitations

The strain profiles presented signify that the small strain assumption is valid since the strains are less than 2%. The governing equation discussed here is only valid for small strains since it is based on the principle of superposition. The beam has been assumed to be slender and the transverse shear effects have been ignored. A solution based on 2D elasticity would be a more accurate way in predicting the deformation and stresses in the beam.

It is seen that the number of layers assumed while approximating the response also affects the quality of the solution. In the n=0.1 case, the material composition changes rapidly from PZT to metal at the PZT end of the beam while in the n=5 case, the material composition changes more rapidly at the metal end of the beam from metal to PZT. The layer thickness is a constant in this study but this is not the best approximation as can be seen by the discontinuity in the strain profiles. It would be more useful to assume thinner layers at the end where the material changes more rapidly. I.e. for n=0.1, it would be better to assume thinner layers at the PZT end and for n=5, it would be better to assume thinner layers at the metal end of the beam.

5.3 Further Research

The following topics are suggested for future research:

1. Finite element solution as well as analytical solution based on 2D elasticity and minimum potential energy approach.

2. Use of high temperature piezoelectric ceramics in such metal-ceramic functionally graded beams to better understand the temperature effects at higher temperatures.

3. Developing and testing such a composite after careful selection of materials

REFERENCES

[1] Uchino K. Piezoelectric actuators and ultrasonic motors. Norwell, MA: Kluwer Academic Publishers; 1997.

[2] Uchino K, Takahashi S. Multilayer ceramic actuators. Current Opinion in Solid State and Materials Science. 1996; 1(5): 698-705.

[3] Uchino K. Piezoelectric actuators 2006. Journal of Electroceramics. 2008; 20(3): 301-311.

[4] Smits JG, Dalke SI, Cooney TK. The constituent equations of piezoelectric bimorphs. Sensors and Actuators A: Physical. 1991; 28(1): 41-61.

[5] Smits JG, Choi W. The constituent equations of piezoelectric heterogeneous bimorphs. Ultrasonics, Ferroelectrics and Frequency Control, IEEE Transactions on. 1991; 38(3): 256-270.

[6] Wang QM, Cross LE. Constitutive equations of symmetrical triple layer piezoelectric benders. Ultrasonics, Ferroelectrics and Frequency Control, IEEE Transactions on. 1999; 46(6): 1343-1351.

[7] Wang QM, Du XH, Xu B, Cross LE. Electromechanical coupling and output efficiency of piezoelectric bending actuators. IEEE Transactions on Ultrasonics, Ferroelectrics and Frequency Control. 1999; 46(3): 638-646.

[8] Steel M, Harrison F, Harper P. The piezoelectric bimorph: An experimental and theoretical study of its quasistatic response. Journal of Physics D: Applied Physics. 1978; 11: 979.

[9] Kugel VD, Chandran S, Cross LE. A comparative analysis of piezoelectric bending-mode actuators. Smart Structures and Materials 1997: Smart Materials Technologies. 1997; 3040: 70-80.

[10] Newnham RE, Bowen L, Klicker K, Cross L. Composite piezoelectric transducers. Materials & Design. 1980; 2(2): 93-106.

[11] Marcus MA. Performance characteristics of piezoelectric polymer flexure mode devices. Ferroelectrics. 1984; 57(1): 203-220.

[12] Kouvatov A, Steinhausen R, Seifert W, Hauke T, Langhammer H, Beige H, et al. Comparison between bimorphic and polymorphic bending devices. Journal of the European Ceramic Society. 1999; 19(6): 1153-1156.

[13] Hauke T, Kouvatov A, Steinhausen R, Seifert W, Beige H, Theo H, et al. Bending behavior of functionally gradient materials. Ferroelectrics. 2000; 238(1): 195-202.

[14] Shi Z, Xiang H, Spencer Jr B. Exact analysis of multi-layer piezoelectric/composite cantilevers. Smart Materials and Structures. 2006; 15: 1447.

[15] Xiang HJ, Shi Z. Electrostatic analysis of functionally graded piezoelectric cantilevers. Journal of Intelligent Material Systems and Structures. 2007; 18(7): 719-726.

[16] Xiang H, Shi Z. Static analysis for functionally graded piezoelectric actuators or sensors under a combined electro-thermal load. European Journal of Mechanics-A/Solids. 2009; 28(2): 338-346.

[17] Taya M, Almajid AA, Dunn M, Takahashi H. Design of bimorph piezo-composite actuators with functionally graded microstructure. Sensors and Actuators A: Physical. 2003; 107(3): 248-260.

[18] Wu C, Kahn M, Moy W. Piezoelectric ceramics with functional gradients: a new application in material design. Journal of the American Ceramic Society. 1996; 79(3): 809-812.

[19] Ying C, Zhifei S. Exact solutions of functionally gradient piezothermoelastic cantilevers and parameter identification. Journal of Intelligent Material Systems and Structures. 2005; 16(6): 531-539.

[20] Huang D, Ding H, Chen W. Piezoelasticity solutions for functionally graded piezoelectric beams. Smart Materials and Structures. 2007; 16: 687.

[21] Takagi K, Li JF, Yokoyama S, Watanabe R. Fabrication and evaluation of PZT/Pt piezoelectric composites and functionally graded actuators. Journal of the European Ceramic Society. 2003; 23(10): 1577-1583.

[22] Zhu X, Meng Z. Operational principle, fabrication and displacement characteristics of a functionally gradient piezoelectric ceramic actuator. Sensors and Actuators A: Physical. 1995; 48(3): 169-176.

[23] Praveen G, Reddy J. Nonlinear transient thermoelastic analysis of functionally graded ceramic-metal plates. International Journal of Solids and Structures. 1998; 35(33): 4457-4476.

[24] Sankar BV, Tzeng JT. Thermal Stresses in Functionally Graded Beams. AIAA journal. 2002; 40(6): 1228-1243.

[25] Reddy J. Analysis of functionally graded plates. International Journal for Numerical Methods in Engineering. 2000; 47(1-3): 663-684.

[26] Cady WG. Piezoelectricity: an introduction to the theory and applications of electromechanical phenomena. 1964.

[27] Ballas R. Piezoelectric multilayer beam bending actuators: Static and dynamic behavior and aspects of sensor integration: Springer-Verlag, Berlin, Heidelberg, New York; 2007.

[28] Zhou D. Experimental investigation of non-linear constitutive behavior of PZT piezoceramics: FZKA; 2003.

[29] Haertling GH. Ferroelectric ceramics: history and technology. Journal of the American Ceramic Society. 1999; 82(4): 797-818.

[30] Leo DJ. Engineering analysis of smart material systems: Wiley Online Library; 2007.

[31] Reddy JN. Mechanics of laminated composite plates and shells: theory and analysis. Boca Raton, FL: CRC Press; 2004.

[32] Reddy JN. An introduction to continuum mechanics: with applications: Cambridge University Press; 2008.

[33] Jaffe H, Berlincourt D. Piezoelectric transducer materials. Proceedings of the IEEE. 1965; 53(10): 1372-1386.

[34] Berlincourt D, Krueger H, Near C. Technical publication TP-226 Properties of Piezoelectricity Ceramics. Morgan electro ceramics. 2003: 12.

[35] Reddy J, Chin C. Thermomechanical analysis of functionally graded cylinders and plates. Journal of Thermal Stresses. 1998; 21(6): 593-626.